Isoliquiritigenin induces apoptosis of human bladder cancer T24 cells via a cyclin-dependent kinase-independent mechanism

LINGLING SI[1*], XINHUI YANG[2*], XINYAN YAN[1], YANMING WANG[1] and QIUSHENG ZHENG[1]

[1]School of Pharmacy, Shihezi University; [2]Department of Pharmacy, The First Affiliated Hospital of the Medical College, Xinjiang Shihezi University, Shihezi, Xinjiang 832002, P.R. China

Abstract. The aim of the present study was to investigate whether an increase in cyclin-dependent kinase 2 (CDK2) activity is involved in apoptosis of human bladder cancer T24 cells induced by isoliquiritigenin (ISL). The viability of T24 cells was estimated using a sulforhodamine B assay. Cell morphological changes were examined using Hoechst 33258 staining. The apoptotic rate was determined by staining cells with Annexin V-fluorescein isothiocyanate and propidium iodide labeling. The mitochondrial membrane potential ($\Delta\Psi_m$) was measured using 5,5',6,6'-tetrachloro-1,1', 3,3'-tetraethyl benzimidazole carbocyanine iodide. Alterations in the apoptosis-related regulators B-cell lymphoma-2 (Bcl-2), Bcl-2-associated X protein (Bax), Bcl-2-interacting mediator of cell death (Bim), apoptotic protease-activating facter-1 (Apaf-1), caspase-9 and caspase-3 were determined using reverse transcription-polymerase chain reaction (PCR) and quantitative PCR methods. Western blot analysis was used to detect the expression of Bcl-2, Bax and caspase-3. CDK2 activity was measured using a spectrometric assay. Following treatment with ISL (between 30 and 70 µg/ml) for 24 h, typical apoptotic morphological changes were observed in T24 cells, exhibiting an edge set of chromosomes, nuclear condensation, nuclear fragmentation and other morphological features.

Correspondence to: Professor Qiusheng Zheng, School of Pharmacy, Shihezi University, 2 North Road, Shihezi, Xinjiang 832002, P.R. China
E-mail: zqsyt@sohu.com

*Contributed equally

Abbreviations: CDK, cyclin-dependent kinase; ISL, isoliquiritigenin; SRB, sulforhodamine B; FITC, fluorescein isothiocyanate; PI, propidium iodide; $\Delta\Psi$m, mitochondrial membrane potential; JC-1, 5,5',6,6'-tetrachloro-1,1',3,3'-tetraethyl benzimidazole carbocyanine iodide; Bcl-2, B-cell lymphoma-2; Bax, Bcl-2-associated X protein; Bim, Bcl-2-interacting mediator of cell death; Apaf-1, apoptotic protease-activating factor-1

Treatment with ISL increased the apoptotic ratio of T24 cells in a concentration-dependent manner and induced a decrease in the $\Delta\Psi_m$ in a time-dependent manner. Treatment with ISL upregulated the expression of Bax, Bim, Apaf-1, caspase-9 and caspase-3, downregulated the expression of Bcl-2, and increased CDK2 activity. MK-8776 (an inhibitor of CDK2) antagonized the apoptosis induced by ISL, and, compared with treatment with ISL alone, pretreatment with MK-8776 inhibited the decrease in $\Delta\Psi_m$, downregulated the mRNA expression of Bax, Bim, Apaf-1, caspase-9 and caspase-3, and upregulated Bcl-2 mRNA expression. Western blot analysis demonstrated that, with increasing ISL concentration, the Bcl-2 expression level was significantly decreased (P<0.05), whereas caspase-3 and Bax expression levels were significantly increased (P<0.01). These results indicated that ISL treatment caused a significant decrease in the proliferation rate and increase in apoptosis of T24 cells. The mechanism by which ISL induces T24 cell apoptosis *in vitro* may be associated with an increase in CDK2 activity, downregulation of the $\Delta\Psi_m$ and activation of caspase-3/caspase-9-mediated mitochondrial apoptotic signaling pathways.

Introduction

To the best of our knowledge, bladder cancer is currently the fourth most common cancer worldwide (1). In China, the incidence of bladder cancer had increased from 1991 to 2009, with >20,000 mortalities in 2009 (2,3). In the United States, there were ~76,000 new cases of bladder cancer and 16,000 bladder cancer-associated mortalities in 2016 (4,5). Currently, although surgical therapies associated with adjuvant chemotherapy following surgery have made marked advances in the treatment of bladder cancer, the rate of recurrence remains high (6). Furthermore, chemotherapy has a high incidence of side effects. Consequently, research into and development of highly efficient and minimally toxic novel drugs is urgently required (7).

Cyclin-dependent kinases (CDKs) are a family of serine/threonine kinases that are required for cell cycle progression, particularly CDK2. CDK2 serves an important role in G_1/S phase transition and S phase progression (8,9). In previous studies, it was also demonstrated that cyclin A-CDK2 activity was markedly upregulated in the early stages of apoptosis and that this upregulation was required for the

progression of apoptosis induced by treatment with ginsenoside Rh2 (10). Nevertheless, the mechanism by which CDK2 functions in the progression of apoptosis in T24 cells induced by isoliquiritigenin (ISL) remains unknown.

Recently, natural products have become one of the important sources in modern drug discovery for its active components with anticancer potential and fewer side effects, particularly for anticancer drugs (6). Licorice is frequently used for culinary purposes in western countries (11-13), and is one of the most commonly used herbs in China for therapeutic effects on different diseases ranging from duodenal ulcers to cancers (14-16). ISL is a natural flavonoid isolated from the root of licorice (*Glycyrrhiza uralensis*). Previous studies have indicated that ISL possesses distinct biological properties, including anti-inflammatory, antioxidant, anti-platelet aggregation, vasorelaxant and estrogenic effects (17-19). A number of studies have demonstrated marked antitumor activities of ISL, including apoptosis induction, cell cycle arrest, migration inhibition and initiation of oxidative stress (20-22). Previous studies have also demonstrated that ISL possesses chemopreventive activities (23-26).

In view of previous studies suggesting an association between CDK2 and apoptosis, the aim of the present study was to determine the effect of MK-8776, an inhibitor of CDK2, on the ISL-induced apoptotic rate in T24 cells. In the present study, the potential underlying molecular mechanism of CDK2 in apoptosis induced by ISL in T24 cells was investigated.

Materials and methods

Reagents. ISL (purity, ≥98%) was obtained from Jiangxi Herb Tiangong Technology Co., Ltd. (Jiangxi, China). Culture medium (RPMI-1640), glutamine and dimethylsulfoxide (DMSO) were purchased from Sigma; Merck KGaA (Darmstadt, Germany). Fetal bovine serum (FBS) was purchased from Tianjin Hao Yang Biological Manufacture Co., Ltd. (Tianjin, China). Penicillin and streptomycin were obtained from Shandong Sunrise Pharmaceutical Co., Ltd. (Shandong, China). MK-8776 was obtained from Selleck Chemicals (Shanghai, China). The CDK2/Cyclin A Kinase Assay kit was obtained from Shanghai Genmed Gene Pharmaceutical Technology Co., Ltd. (Shanghai, China). Primary antibodies against β-actin (catalog no. sc-130300), B cell lymphoma 2 (Bcl-2) (catalog no. sc-130308), caspase-3 (catalog no. sc-56052) and Bcl-2 associated X factor (Bax; catalog no. sc-80658) were purchased from Santa Cruz Biotechnology, Inc. (Dallas, TX, USA). Unless indicated otherwise, other reagents were purchased from Sigma; Merck KGaA. All other chemicals were of analytical grade.

Cell culture and treatment. T24 cells were purchased from the Cell Bank of the Committee on Type Culture Collection of the Chinese Academy of Sciences (Shanghai, China). The cells were maintained in RPMI-1640 medium supplemented with 10% (v/v) FBS, 100 U/ml penicillin and 100 μg/ml streptomycin at 37˚C in a humidified atmosphere containing 5% CO_2. Cells were allowed to attach for 24 h before treatment. ISL was dissolved in DMSO and diluted with fresh medium to achieve the desired concentration. The final concentration of DMSO was <0.2% in the fresh medium,

and DMSO at this concentration exhibited no significant effect on cell viability.

Cell viability assay. The T24 cells were trypsinized and seeded into 96-well plates at $8x10^4$ cells/ml. Subsequently, the cells were exposed to ISL (0, 15, 30, 45, 60 and 75 μg/ml) at 37˚C for 24 h followed by further incubation in fresh medium at 37˚C for another 24 h. The effect of ISL-induced cytotoxicity was evaluated using a sulforhodamine B (SRB) assay as described previously (27). The optical density (OD) was determined at a wavelength of 490 nm. The inhibition ratio was calculated as follows.

$$\text{Inhibition ratio (\%)} \left(1 - \frac{\text{OD of cells cultured with ISL}}{\text{OD of control}} \right) \times 100$$

Trypan blue exclusion assay. The lethality of ISL on T24 cells was determined using a trypan blue exclusion assay. After 24 h of incubation with 0, 15, 30, 45, 60 and 75 μg/ml ISL at 37˚C, T24 cells were removed from the culture medium and cells that excluded trypan blue were counted in a Neubauer chamber using a light microscope. The lethal ratio was calculated as follows.

$$\text{Lethal ratio (\%)} = \frac{\text{Dead cell count}}{\text{Total cell count}} \times 100$$

Hoechst 33258 staining. The T24 cells were seeded in 6-well culture dishes ($2x10^5$ cells/well). Following treatment with ISL at 0, 30, 50 and 70 μg/ml at 37˚C for 24 h, the cells were fixed with Carnoy's fixative consisting of methanol and glacial acetic acid (3:1, v/v), washed twice with PBS, stained with Hoechst 33258 (5 mg/ml) for 5 min in the dark, as described previously (28), and washed extensively three times with PBS. Nuclear staining was examined using a fluorescence microscope (Nikon LH-M100CB; Jirui Co., Ltd., Suzhou, China) and images were captured using Image-Pro Plus Premier (version 9.1.4; Media Cybernetics, Inc., Rockville, MD, USA). Cells that exhibited decreased nuclear size, chromatin condensation, intense fluorescence and nuclear fragmentation were considered apoptotic.

Analysis of apoptosis by Annexin V-fluorescein isothiocyanate (FITC) and propidium iodide (PI). The cells ($2x10^5$ cells/well) were pretreated with 0.16 μM MK-8776 at 37˚C for 1 h, incubated with ISL at 0, 30, 50 and 70 μg/ml at 37˚C for 24 h and harvested. Specific binding of Annexin V-FITC was carried out by incubating the cells at room temperature for 15 min in a binding buffer containing a saturating concentration of Annexin V-FITC and PI, as described previously (29). Following incubation, the cells were quantified using a flow cytometer (BD Biosciences, Franklin Lakes, NJ, USA) and analyzed using CellQuest Pro acquisition software (version 4.0; FACS Calibur; BD Biosciences, San Jose, CA, USA).

Detection of mitochondrial membrane potential ($\Delta\Psi_m$) using 5,5',6,6'-tetrachloro-1,1',3,3'-tetraethyl benzimidazole carbocyanine iodide (JC-1). Following reaching optimal confluence, cells were pretreated with 0.16 μM MK-8776 for 1 h, and incubated with 50 μg/ml ISL at 37˚C for 24 h. In addition, the cells not pretreated with MK-8776 at 0.16 μM were incubated with ISL at 0, 30, 50 and 70 μg/ml at 37˚C for 4, 8, 16 and 24 h washed with ice-cold PBS, exposed to 500 μl JC-1

Table I. Primer sequences.

Gene	Primer	T_m, °C
Bcl-2	Forward: 5'-GGAAATATGGCGCACGCT-3' Reverse: 5'-TCACTTGTGGCCCA-3'	59
Bax	Forward: 5'-ACGAACTGGACAGTAACATGGAG-3' Reverse: 5'-CAGTTTGCTGGCAAAGTAGAAAAG-3'	59
Bim	Forward: 5'-CACATGAGCACATTTCCCTCT-3' Reverse: 5'-AAGGCACAAAACCTGCAGTAA-3'	57
Apaf-1	Forward: 5'-TGGAATGGCAGGCTGTGGGA-3' Reverse: 5'-TGCACTCCCCCTGGGAAACA-3'	62
Caspase-9	Forward: 5'-ACGCGTTACTGGCATTGAGG-3' Reverse: 5'-CAGTGGGCTCACTCTGAAGACC-3'	62
Caspase-3	Forward: 5'-CTGGACTGTGGCATTGAGAC-3' Reverse: 5'-ACAAAGCGACTGGATGAACC-3'	59
GAPDH	Forward: 5'-CAAGGTCATCCATGACAACTTTG-3' Reverse: 5'-GTCCACCACCCTGTTGCTGTAG-3'	57

T_m, melting temperature. Bcl-2, B-cell lymphoma-2; Bax, Bcl-2-associated X protein; Bim, Bcl-2-interacting mediator of cell death; Apaf-1, apoptotic protease-activating factor-1.

dye and incubated in the dark at 37°C for 20 min. Following washing three times with incubation buffer (Nanjing KeyGen Biotech Co., Ltd., Nanjing, China), the cells were diluted in 500 μl incubation buffer and the fluorescence intensity of the cells was analyzed using a FACScan flow cytometer (BD Biosciences). Fluorescence at excitation/emission wavelengths of 485/580 nm (red) and 485/530 nm (green) was read using a fluorescence plate reader (Varioskan Flash 3001; Thermo Fisher Scientific, Inc., Waltham, MA, USA).

Reverse transcription-polymerase chain reaction (RT-PCR) and quantitative PCR (qPCR). RT-PCR and qPCR (30,31) were performed to examine the mRNA expression of B-cell lymphoma-2 (Bcl-2), Bcl-2-associated X protein (Bax), Bcl-2-interacting mediator of cell death (Bim), apoptotic protease-activating factor-1 (Apaf-1), caspase-9 and caspase-3. The primer sequences are presented in Table I. The cells were pretreated with 0.16 μM MK-8776 at 37°C for 1 h and incubated with 50 μg/ml ISL at 37°C for 24 h. The cells were further incubated with 0, 30, 50 and 70 μg/ml ISL at 37°C for 24 h and harvested. Total RNA was extracted from the T24 cells using TRIzol reagent (Shanghai Sangong Biotech Co., Ltd. (Shanghai, China) and quality was determined according to the A_{260}/A_{280} ratio. cDNA synthesis was performed using a RevertAid First Strand cDNA Synthesis kit (Thermo Fisher Scientific, Inc.), according to the manufacturer's protocol. Subsequently, the synthesized cDNA was amplified. The cycling conditions were set as indicated by Sangong Biotech Co. Ltd. The reaction mixture contained 12.5 μl 2X PCR Master mix (Sangong Biotech Co., Ltd.), 3 μl cDNA template and 0.5 μl each primer. The cycling conditions used were as follows: 95°C for 5 min, followed by 37 cycles of 94°C for 30 sec, heating at specified melting temperature (T_m, Table I) for 30 sec, 72°C for 30 sec and 72°C for 5 min. cDNA products were analyzed using 2% agarose gel electrophoresis. Three independent experiments were performed. Images were captured using Image-Pro Plus Premier (version 9.1.4; Media Cybernetics, Inc., Rockville, MD, USA).

Relative gene expression was quantified using qPCR with a SYBR Green kit (Rotor-Gene Q; Qiagen, Inc. Valencia, CA, USA), enabling detection of PCR products, according to the manufacturer's protocol. The cDNA was amplified using qPCR with the primer pairs given in Table I (synthesized by Sangon Biotech Co., Ltd.). The cycling conditions were as follows: 95°C for 5 min, followed by 40 cycles of 95°C for 30 sec, T_m (see Table I) for 30 sec, and 72°C for 30 sec. A total of three independent experiments were performed. Quantitative data was analyzed using the Sequence Detection system software (version 1.0; Applied Biosystems; Thermo Fisher Scientific, Inc.). The relative quantity of target mRNA was determined using the $2^{-\Delta\Delta Cq}$ method (32). Each sample was analyzed using GAPDH as an endogenous reference gene for mRNA normalization.

CDK2 activity assay. T24 cells were seeded at a density of 2.5×10^5 cells/ml in flasks and incubated at 37°C for 24 h. The cells were pretreated with 0.16 μM MK-8776 at 37°C for 1 h and incubated with 50 μg/ml ISL at 37°C for 24 h. The cells were further incubated with ISL at 0, 30, 50 and 70 μg/ml at 37°C for 4, 8, 16 and 24 h. Following the addition of 2 ml cleanup solution (CDK2/cyclin A kinase assay reagent A; Shanghai Genmed Gene Pharmaceutical Technology Co., Ltd., Shanghai, China) and protein extraction, the CDK2/cyclin A kinase assay kit (Shanghai Genmed Gene Pharmaceutical Technology Co., Ltd.) was used to determine CDK2 activity, according to the manufacturer's protocol. Experiments were performed in triplicate.

Western blot analysis. The cells were harvested, extracted with cell lysis buffer (catalog no. R0010; Beijing Solarbio Science & Technology Co., Ltd., Beijing, China) and
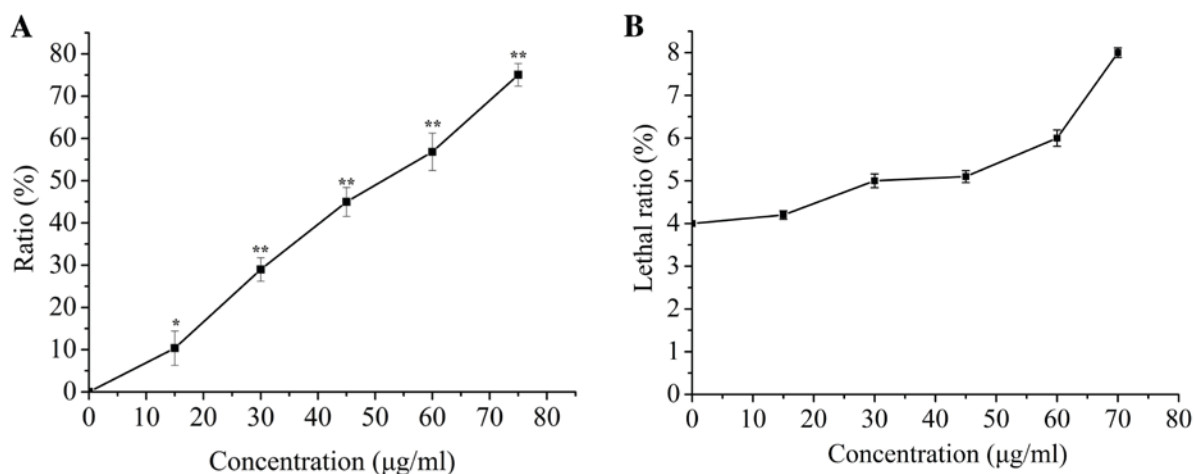
Figure 1. Effect of ISL on T24 cell proliferation and survival. (A) The inhibition ratio of cell proliferation was determined using a sulforhodamine B assay and (B) the lethal ratio was determined using a trypan blue exclusion test following incubation with ISL at the concentrations indicated for 24 h. Results are presented as the mean ± standard deviation of three independent experiments. $^*P<0.05$; $^{**}P<0.01$ vs. untreated control group cells. ISL, isoliquiritigenin.

centrifuged at 12,000 x g for 5 min at 4°C. Protein concentration was determined using a bicinchoninic acid assay kit (catalog no. PC0020; Beijing Solarbio Science & Technology Co., Ltd.). The protein lysates were diluted to equal concentrations and heated at 100°C for 5 min. Soluble lysates (15 μl/lane) were subjected to SDS-PAGE (10% gel), transferred onto nitrocellulose membranes (GE Healthcare Bio-Sciences, Pittsburgh, PA, USA) and blocked with 5% non-fat milk in Tris-buffered saline with Tween-20 (TBST) for 2 h at room temperature. The membranes were incubated with the anti-β-actin (mouse anti-human; 1:5,000), anti-Bcl-2 (monoclonal, mouse anti-human; 1:500), anti-caspase-3 (monoclonal, mouse anti-human; 1:500) and anti-Bax (monoclonal, mouse anti-human; 1:400) at 4°C overnight and incubated with horseradish peroxidase-conjugated secondary antibody (goat anti-mouse, 1:5,000; catalog no. HS201; Beijing TransGen Biotech Co., Ltd., Beijing, China). Western blots were developed using enhanced chemiluminescence (ECL, Thermo Fisher Scientific, Inc.) and exposed on radiographic film (Kodak, Rochester, NY, USA). Densitometric analysis was performed using Image Quant LAS 4000 (Amersham, Buckinghamshire, UK), and the autoradiographs were quantified using ImageJ software (version 1.49n; National Institutes of Health, Bethesda, Maryland, USA). Three independent experiments were performed.

Statistical analysis. All results were obtained by ≥3 independent experiments. The data are expressed as the mean ± standard deviation. One-way analysis of variance was performed, and the mean values were compared using Fisher's multiple comparison test. All statistical analyses were performed using Minitab for Windows (version 16; Minitab Inc., PA, USA). P<0.05 was considered to indicate a statistically significant difference.

Results

ISL treatment inhibits proliferation of T24 cells. The effect of ISL-induced cytotoxicity was determined using an SRB assay. At 24 h following ISL treatment, cell proliferation decreased with increasing concentrations of ISL, and the half-maximal inhibitory concentration was ~50 μg/ml (Fig. 1A). However, the SRB assay did not reveal whether the decrease in cell proliferation was associated with cell death or an apparent loss of viability. To solve this problem, a trypan blue exclusion test was performed on T24 cells treated with ISL. ISL (<75 μg/ml) did not significantly affect the lethality ratio of T24 cells (Fig. 1B), which indicated that the inhibitory effect of ISL on cell proliferation was not due to direct killing of T24 cells and identified that no significant cytotoxicity was observed compared with the control.

Nuclear morphology. Morphological changes were examined by Hoechst 33258 staining. T24 cells were treated with ISL for 24 h, and evident apoptotic morphological changes were observed. In the control group, the nuclei of T24 cells were round and homogeneously stained (Fig. 2), whereas ISL-treated cells exhibited evident apoptotic characteristics including cell shrinkage, loss of membrane integrity or deformation, nuclear fragmentation and chromatin compaction of late apoptotic appearance.

Assessment of apoptotic cells. Apoptosis was determined by staining cells with Annexin V-FITC and PI. A concentration-dependent increase in the apoptotic ratio of T24 cells was demonstrated by Annexin V and PI staining using flow cytometry (Fig. 3). After 24 h of incubation, there were limited numbers of apoptotic cells in the control group (5.57±2.89%), whereas in the 30, 50 and 70 μg/ml ISL treatment groups, the proportion of apoptotic cells was 19.72±2.03, 35.3±1.93 and 59.77±3.09%, respectively.

Effects of ISL on the $\Delta\Psi_m$ of the cells. Mitochondria serve an important role in the regulation of apoptosis, and apoptosis mediated by the mitochondrial signaling pathway is often associated with a decrease in $\Delta\Psi_m$. The $\Delta\Psi_m$ changes in T24 cells were determined by staining with JC-1 dye following various treatment periods, and detection using flow cytometry and fluorescence microscopic analysis. The decrease in intensity of JC-1 dye staining reflected a decrease in the $\Delta\Psi_m$.
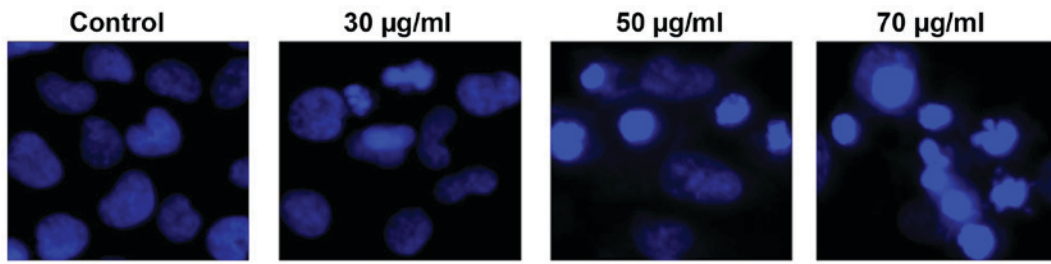
Figure 2. Hoechst 33258 staining of T24 cells following treatment with isoliquiritigenin at the concentrations indicated for 24 h. Fluorescence images were captured following Hoechst 33258 staining (magnification, x200).
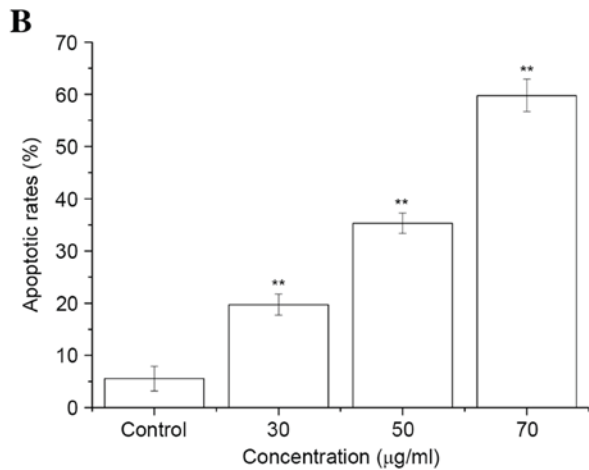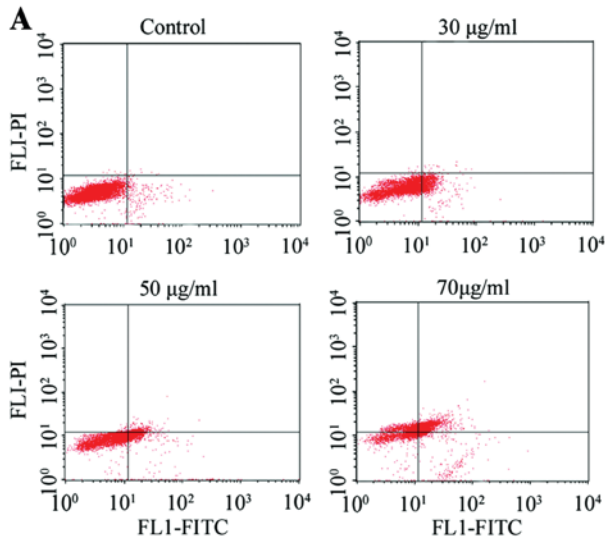

Figure 3. Effect of ISL on apoptotic rates in T24 cells. Cells were treated with ISL at 0, 30, 50 and 70 µg/ml for 24 h, permeabilized, stained with Annexin V, and kept on ice until analysis using flow cytometry. (A) Cells in the lower left quadrant were alive, cells in the lower right quadrant were in early apoptosis, cells in the upper right quadrant were in late apoptosis and cells in the upper left quadrant were dead. (B) Quantification of apoptotic rates. Results are presented as the mean ± standard deviation of three separate experiments. **P<0.01 vs. untreated control group cells. ISL, isoliquiritigenin; FITC, fluorescein isothiocyanate; PI, propidium iodide.
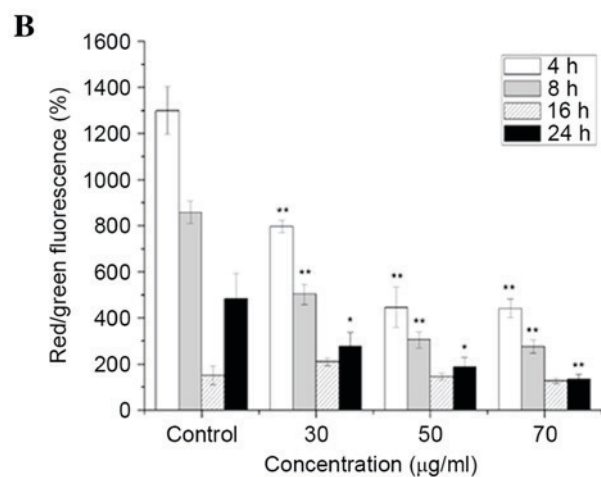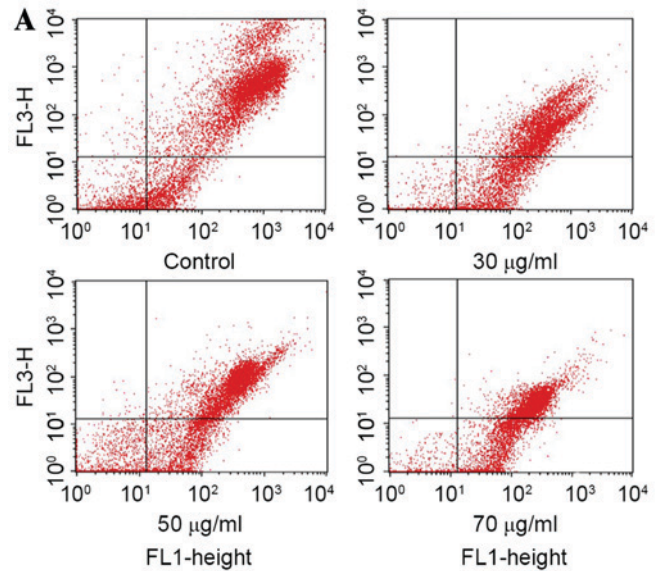
Figure 4. ISL decreases the mitochondrial membrane potential in T24 cells. Cells were incubated with ISL at 0, 30, 50 and 70 µg/ml for various periods of time, and treated with JC-1 dye. (A) The retention of JC-1 dye was determined using flow cytometry. (B) Quantitative analysis of cell cycle distribution. Results are presented as the mean ± standard deviation of three independent experiments. *P<0.05; **P<0.01 vs. untreated control group cells. ISL, isoliquiritigenin.

As presented in Fig. 4, a concentration- and time-dependent decrease in $\Delta\Psi_m$ was observed in ISL-treated cells.

ISL increases the mRNA expression of Bax, Bim, Apaf-1, caspase-9 and caspase-3, and decreases the mRNA expression of Bcl-2 in T24 cells. The mRNA expression levels of Bax, Bim, Apaf-1, caspase-9 and caspase-3 were significantly increased, and that of Bcl-2 was significantly decreased in ISL-treated T24 cells in a concentration-dependent manner (P<0.05 or <0.01; Fig. 5).
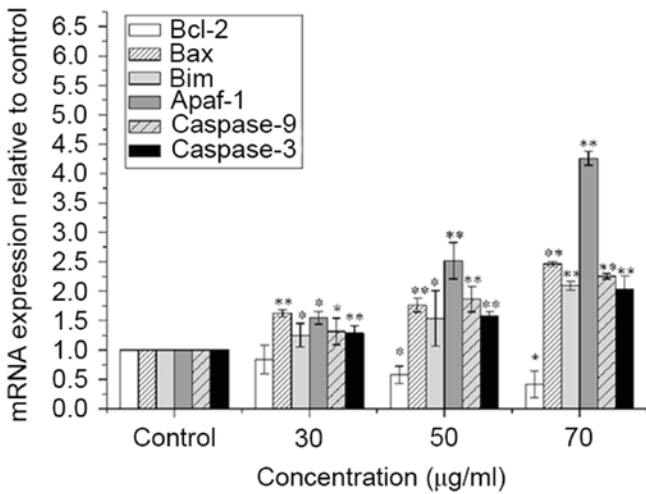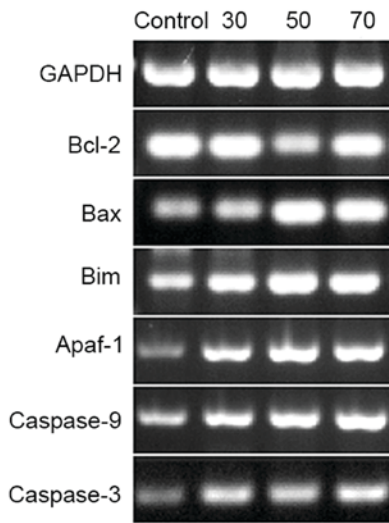
Figure 5. mRNA expression of Bcl-2, Bax, Bim, Apaf-1, caspase-9 and caspase-3 in T24 cells treated with isoliquiritigenin at the concentrations indicated (μg/ml). mRNA expression was determined using the reverse transcription-polymerase chain reaction and agarose gel electrophoresis. Quantification results are presented as the mean ± standard deviation of three independent experiments. *P<0.05; **P<0.01 vs. untreated control group cells. Bcl-2, B-cell lymphoma 2; Bax, Bcl-2-associated X protein; Bim, Bcl-2-interacting mediator of cell death; Apaf-1, apoptotic protease-activating factor-1.
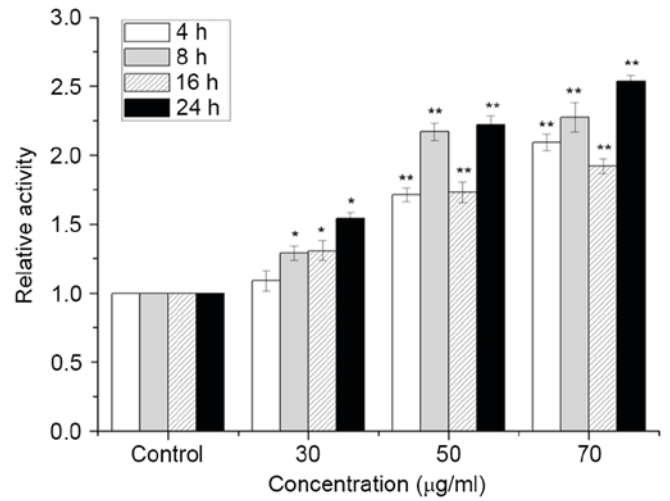

Figure 6. Effect of isoliquiritigenin on cyclin-dependent kinase 2 activity. Results are presented as the mean ± standard deviation of three independent experiments. *P<0.05; **P<0.01 vs. untreated control group cells.
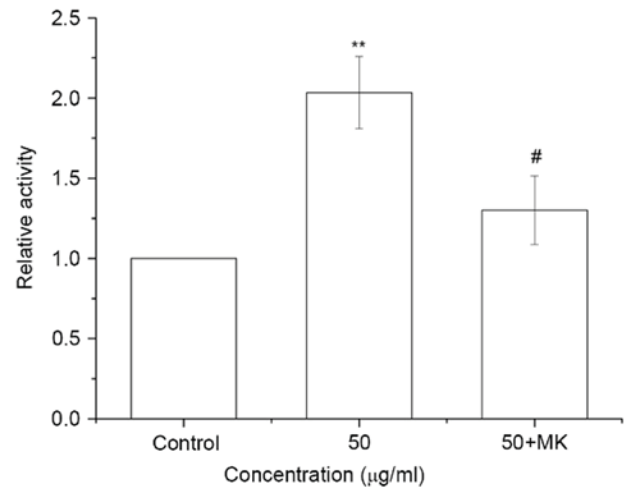

Figure 7. Effect of MK-8776 on CDK2 activity in ISL-treated T24 cells. T24 cells pretreated or not with MK-8776 were treated with ISL at 50 μg/ml and CDK2 activity was determined. Results are the mean ± standard deviation of three independent experiments. **P<0.01 vs. untreated control group cells; #P<0.05 vs. 50 μg/ml ISL-treated group cells. CDK2, cyclin-dependent kinase 2; ISL, isoliquiritigenin; MK, MK-8776.

ISL increases the activity of CDK2 in T24 cells. As presented in Fig. 6, CDK2 activity was increased significantly following treatment with ISL compared with that of the control (P<0.05). The maximum enhancement in CDK2 activity was observed following treatment with 70 μg/ml ISL at all time points.

MK-8776 reverses the ISL-induced increase in CDK2 activity in T24 cells. The cells were pretreated with 0.16 μM MK-8776 at 37˚C for 1 h and incubated with ISL at 50 μg/ml at 37˚C for 24 h. CDK2 activity was significantly increased in ISL-treated cells (P<0.01), whereas CDK2 activity in ISL-treated cells was significantly decreased by pretreatment with MK-8776 for 1 h compared with ISL-treated cells without MK-8776 pre-treatment (P<0.05; Fig. 7).

MK-8776 decreases the apoptotic ratio induced by ISL in T24 cells. The cells were pretreated with 0.16 μM MK-8776

at for 1 h and incubated with 50 μg/ml ISL for 24 h. The apoptotic ratio of T24 cells was significantly increased by ISL treatment at 50 μg/ml for 24 h, whereas the apoptotic ratio of ISL-treated cells was significantly decreased by pretreatment with MK-8776 for 1 h compared with ISL-treated cells not pretreated with MK-8776 (P<0.01; Fig. 8).

MK-8776 reverses the ISL-induced decrease in the $\Delta\Psi_m$ in T24 cells. ISL treatment at 50 μg/ml for 24 h led to a significant decrease in $\Delta\Psi_m$ in T24 cells, whereas pretreatment with MK-8776 for 1 h significantly reversed the decrease in $\Delta\Psi_m$ induced by ISL in T24 cells (P<0.01; Fig. 9).

MK-8776 reverses the increases in Bax, Bim, Apaf-1, caspase-9 and caspase-3 mRNA expression, and the decrease in Bcl-2 mRNA expression in T24 cells induced by
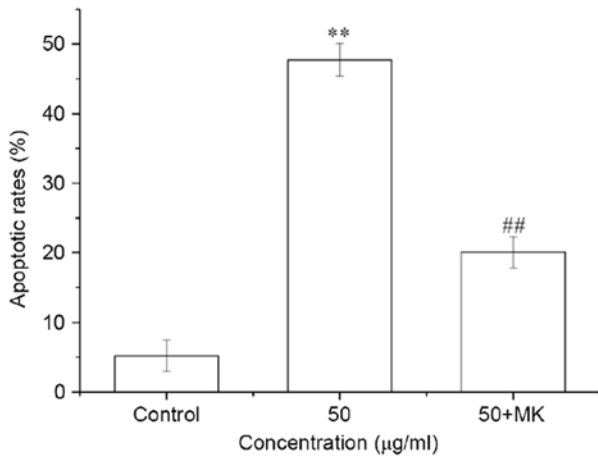
Figure 8. Effect of the CDK2 inhibitor MK-8776 on the apoptotic ratio. T24 cells pretreated or not with MK-8776 were treated with ISL at 50 μg/ml and CDK2 activity was determined. Results are the mean ± standard deviation of three independent experiments. **P<0.01 vs. untreated control group cells; $^{\#\#}$P<0.01 vs. 50 μg/ml ISL-treated group cells. CDK2, cyclin-dependent kinase 2; ISL, isoliquiritigenin; MK, MK-8776.
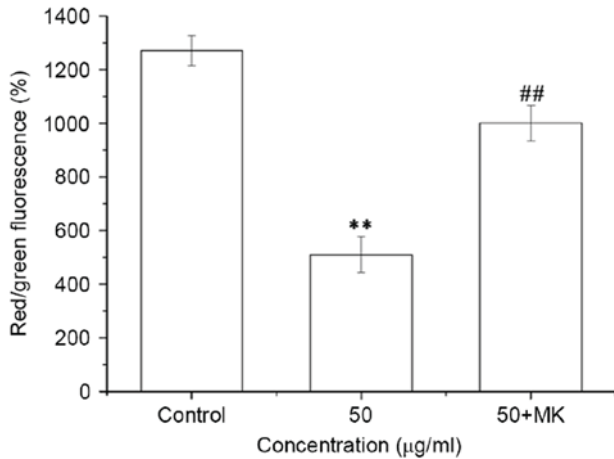

Figure 9. Effect of the cyclin-dependent kinase 2 inhibitor MK-8776 on $\Delta\Psi_m$. T24 cells pretreated or not with MK-8776 were treated with ISL at 50 μg/ml and the $\Delta\Psi_m$ was determined. Results are presented as the mean ± standard deviation of three independent experiments. **P<0.01 vs. untreated control group cells; $^{\#\#}$P<0.01 vs. 50 μg/ml ISL-treated group cells. $\Delta\Psi_m$, mitochondrial membrane potential; ISL, isoliquiritigenin; MK, MK-8776.

ISL treatment. Pretreatment with MK-8776 for 1 h led to a reversal of the decrease in the mRNA expression level of anti-apoptotic Bcl-2, and of the increase in the mRNA expression of proapoptotic Bax, Bim, Apaf-1, caspase-9 and caspase-3 induced by treatment with ISL at 50 μg/ml (P<0.05 or <0.01; Fig. 10).

ISL increases the protein expression of Bax and caspase-3, and decreases the expression of Bcl-2 in T24 cells. To further investigate the potential underlying molecular mechanism of ISL-induced apoptosis, the protein levels of Bcl-2, Bax and caspase-3 were determined by western blot analysis. It was observed that the Bcl-2 expression level was decreased, and the Bax and caspase-9 expression levels were increased, in a ISL concentration-dependent manner. Compared with the ISL-treated cells alone, pretreatment with MK-8776 led to
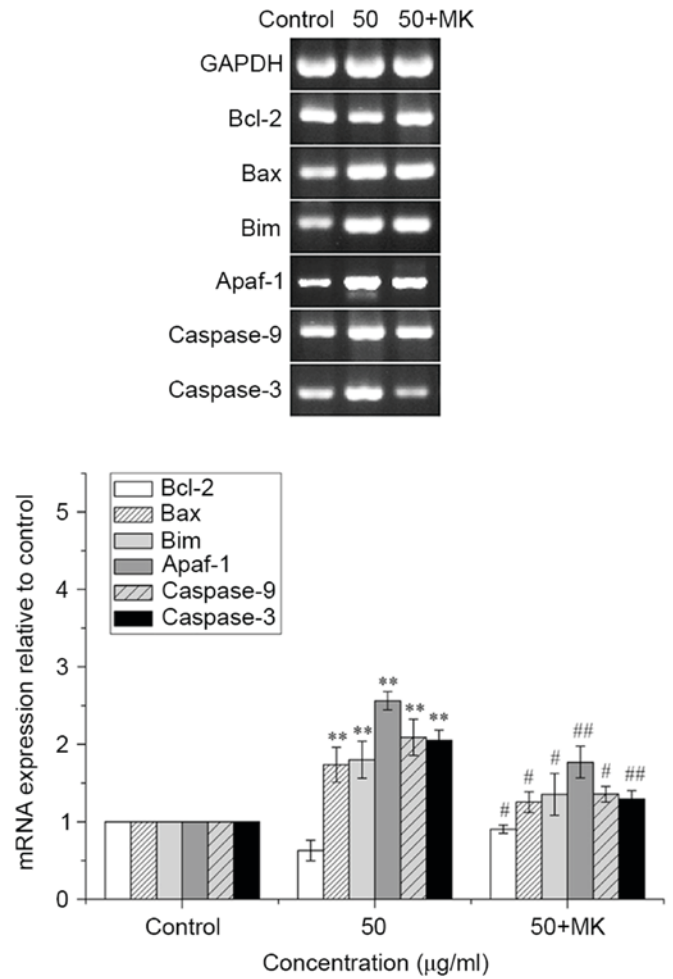

Figure 10. MK-8776 antagonizes the increases in Bax, Bim, Apaf-1, caspase-9 and caspase-3 mRNA expression, and the decrease in Bcl-2 mRNA expression in T24 cells. T24 cells pretreated or not with MK-8776 were treated with ISL at 50 μg/ml and mRNA expression was determined using the reverse transcription-polymerase chain reaction and agarose gel electrophoresis. Quantification results are presented as the mean ± standard deviation of three independent experiments. **P<0.01 vs. untreated control group cells; $^{\#}$P<0.05, $^{\#\#}$P<0.01 vs. 50 μg/ml ISL-treated group cells. Bax, Bcl-2-associated X protein; Bim, Bcl-2-interacting mediator of cell death; Apaf-1, apoptotic protease-activating factor-1; Bcl-2, B-cell lymphoma 2; ISL, isoliquiritigenin.

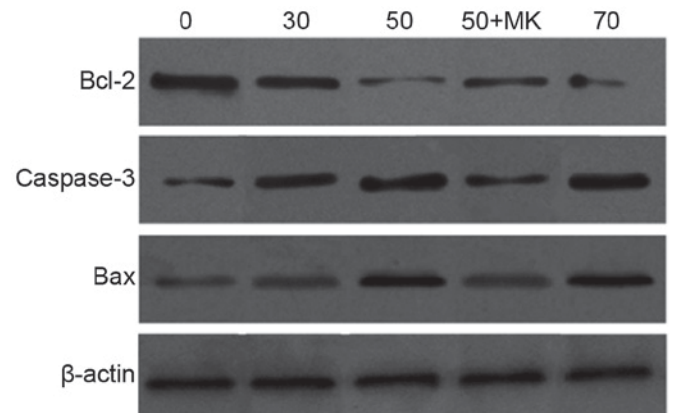
Figure 11. Effects of ISL on Bcl-2, Bax and caspase-3 protein expression. Protein levels of Bcl-2, caspase-3 and Bax following ISL treatment at the concentrations indicated (μg/ml) with or without MK-8776 pretreatment were examined by western blot analysis. β-actin was used as a loading control. ISL, isoliquiritigenin; Bcl-2, B-cell lymphoma 2; Bax, Bcl-2-associated X protein; MK, MK-8776.

an increase in the level of antiapoptotic Bcl-2 mRNA, and a decrease in the level of the proapoptotic Bax and caspase-3 (active form with minor molecular mass) (Fig. 11).

Discussion

Although ISL has been implicated in the induction of apoptosis in a variety of cell types (33-37), the underlying molecular mechanism by which ISL induces apoptosis remains unclear. In particular, the signaling pathway by which ISL induces apoptosis in T24 cells remains unknown. The alteration in mitochondrial membrane depolarization is intimately associated with apoptosis, which indicates that the ISL-mediated arrest of proliferation has an association with T24 cell apoptosis. Prosurvival Bcl-2 family members localized in the outer membrane of the mitochondria are important regulatory factors in the process of cell apoptosis. Bcl-2 family members are divided into two groups: Antiapoptotic proteins, including Bcl-2, B-cell lymphoma extra large and B-cell lymphoma W, and proapoptotic proteins, including Bcl-2 antagonist/killer, Bax, Bcl-2-associated death promoter and Bim. The balance of these two groups determines the status of cells as alive or dead (38,39). First, proapoptotic proteins open the permeability transition pore on the mitochondrial membrane and promote the release of cytochrome *c* which combines with Apaf-1. Secondly, procaspase-9 is activated, and caspase-3, downstream of the activator caspases, is activated through the mitochondrial signaling pathway. Finally, activation of these signaling pathways leads to cell apoptosis. In the present study, following treatment of T24 cells with various concentrations of ISL, a decrease in the $\Delta\Psi_m$ was induced in a time-dependent manner. In addition, ISL significantly upregulated the activities of the related apoptotic signaling molecules Bax, Bim, Apaf-1, caspase-9 and caspase-3, and downregulated the activation of Bcl-2. Furthermore, the results of the present study identified that ISL treatment upregulated the pro-apoptotic proteins Bax and caspase-3, and downregulated the anti-apoptotic protein Bcl-2. These results suggested that ISL induced apoptosis of T24 cells by a molecular mechanism responsible for depolarization of $\Delta\Psi_m$, and that ISL led to the apoptosis of T24 cells via mitochondrial signaling pathways.

The association of CDK2 and cyclin E/cyclin A allows progression through G_1 phase and entry into DNA synthesis, which are associated with cell cycle regulation (39-41). Besides being important proteins of cell cycle regulation, CDK2 and cyclin A are involved in the apoptotic process. It has been demonstrated that upregulation of CDK2 activity is required for etoposide-induced apoptosis in human cervical carcinoma HeLa cells and mitochondrial translocation of Bax, as well as the decrease in $\Delta\Psi_m$ (38). In order to determine whether CDK2 serves a vital role in ISL-induced apoptosis in T24 cells, T24 cells were treated with various concentrations of ISL, and the activity of CDK2 increased in a time-dependent manner, whereas the activity of CDK2 was decreased by pretreatment with MK-8776 in the ISL-treated cells.

In order to determine whether CDK2 is involved in ISL-induced apoptosis in T24 cells, the effect of MK-8776 on ISL-induced apoptosis was investigated. The apoptotic ratio was decreased markedly in the MK-8776 treatment group. Furthermore, MK-8776 inhibited the decrease in $\Delta\Psi_m$ and downregulated the mRNA expression of Bax, Bim, Apaf-1, caspase-9 and caspase-3, and upregulated the expression of Bcl-2. In addition, compared with the ISL-treated alone, the level of antiapoptotic Bcl-2 mRNA increased, and the mRNA expression of proapoptotic protein Bax and caspase-3 was decreased by pretreatment with MK-8776, suggesting that CDK2 served an important role in ISL-induced apoptosis. The apoptotic mechanism may be associated with CDK2-mediated depolarization of $\Delta\Psi_m$ (42-44), which initiates a caspase cascade by facilitating a decrease in $\Delta\Psi_m$ and finally leading to mitochondrial apoptosis.

ISL induced apoptosis in T24 cells. CDK2 activation was the critical step, which induced irreversible apoptotic cell death in the cells. However, the regulatory molecular mechanism for CDK2 activity in association with ISL-induced apoptotic pathway remains unclear.

References

1. Huang W, Chen Y, Liu Y, Zhang Q, Yu Z, Mou L, Wu H, Zhao L, Long T, Qin D and Gui Y: Roles of ERβ and GPR30 in proliferative response of human bladder cancer cell to estrogen. Biomed Res Int 2015: 251780, 2015.
2. Yee DS, Ishill NM, Lowrance WT, Herr HW and Elkin EB: Ethnic differences in bladder cancer survival. Urology 78: 544-549, 2011.
3. Parkin DM: International variation. Oncogene 23: 6329-6340, 2004.
4. Braithwaite D, Demb J, Henderson LM, Mandelblatt JS and Kerlikowske K: American Cancer Society: Cancer Facts & Figures, 2016.
5. Douglass L and Schoenberg M: The future of intravesical drug delivery for non-muscle invasive bladder cancer. Bladder Cancer 2: 285-292, 2016.
6. Jiang J, Yuan X, Zhao H, Yan X, Sun X and Zheng Q: Licochalcone A inhibiting proliferation of bladder cancer T24 cells by inducing reactive oxygen species production. Biomed Mater Eng 24: 1019-1025, 2014.
7. Stein JP and Skinner DG: Radical cystectomy for invasive bladder cancer: Long-term results of a standard procedure. World J Urol 24: 296-304, 2006.
8. Peng C, Zeng W, Su J, Kuang Y, He Y, Zhao S, Zhang J, Ma W, Bode AM, Dong Z and Chen X: Cyclin-dependent kinase 2 (CDK2) is a key mediator for EGF-induced cell transformation mediated through the ELK4/c-Fos signaling pathway. Oncogene 35: 1170-1179, 2016.
9. Hu JW, Sun P, Zhang DX, Xiong WJ and Mi J: Hexokinase 2 regulates G1/S checkpoint through CDK2 in cancer-associated fibroblasts. Cell Signal 26: 2210-2216, 2014.
10. Jin YH, Yim H, Park JH and Lee SK: Cdk2 activity is associated with depolarization of mitochondrial membrane potential during apoptosis. Biochem Biophys Res Commun 305: 974-980, 2003.
11. Kinghorn AD, Pan L, Fletcher JN and Chai H: The relevance of higher plants in lead compound discovery programs. J Nat Prod 74: 1539-1555, 2011.
12. Fintelmann V: Modern phytotherapy and its uses in gastrointestinal conditions. Planta Med 57 (Suppl 7): S48-S52, 1991.
13. Madak-Erdogan Z, Gong P, Zhao YC, Xu L, Wrobel KU, Hartman JA, Wang M, Cam A, Iwaniec UT, Turner RT, *et al*: Dietary licorice root supplementation reduces diet-induced weight gain, lipid deposition, and hepatic steatosis in ovariectomized mice without stimulating reproductive tissues and mammary gland. Mol Nutr Food Res 60: 369-380, 2016.
14. Fukai T, Marumo A, Kaitou K, Kanda T, Terada S and Nomura T: Anti-*Helicobacter pylori* flavonoids from licorice extract. Life Sci 71: 1449-1463, 2002.
15. Funakoshi-Tago M, Nakamura K, Tsuruya R, Hatanaka M, Mashino T, Sonoda Y and Kasahara T: The fixed structure of Licochalcone A by alpha, beta-unsaturated ketone is necessary for anti-inflammatory activity through the inhibition of NF-kappaB activation. Int Immunopharmacol 10: 562-571, 2010.
16. Xiao XY, Hao M, Yang XY, Ba Q, Li M, Ni SJ, Wang LS and Du X: Licochalcone A inhibits growth of gastric cancer cells by arresting cell cycle progression and inducing apoptosis. Cancer Lett 302: 69-75, 2011.

17. Kim YM, Kim TH, Kim YW, Yang YM, Ryu DH, Hwang SJ, Lee JR, Kim SC and Kim SG: Inhibition of liver X receptor-α-dependent hepatic steatosis by isoliquiritigenin, a licorice antioxidant flavonoid, as mediated by JNK1 inhibition. Free Radic Biol Med 49: 1722-1734, 2010.

18. Yadav VR, Prasad S, Sung B and Aggarwal BB: The role of chalcones in suppression of NF-κB-mediated inflammation and cancer. Int Immunopharmacol 11: 295-309, 2011.

19. Chin YW and Kinghorn AD: Structural characterization, biological effects, and synthetic studies on xanthones from mangosteen (*Garcinia mangostana*), a popular botanical dietary supplement. Mini Rev Org Chem 5: 355-364, 2008.

20. Wang Z, Wang N, Liu P, Chen Q, Situ H, Xie T, Zhang J, Peng C, Lin Y and Chen J: MicroRNA-25 regulates chemoresistance-associated autophagy in breast cancer cells, a process modulated by the natural autophagy inducer isoliquiritigenin. Oncotarget 5: 7013-7026, 2014.

21. Zhao H, Yuan X, Li D, Chen H, Jiang J, Wang Z, Sun X and Zheng Q: Isoliquiritigen enhances the antitumour activity and decreases the genotoxic effect of cyclophosphamide. Molecules 18: 8786-8798, 2013.

22. Haraguchi H, Ishikawa H, Mizutani K, Tamura Y and Kinoshita T: Antioxidative and superoxide scavenging activities of retrochalcones in *Glycyrrhiza inflata*. Bioorg Med Chem 6: 339-347, 1998.

23. Fukai T, Satoh K, Nomura T and Sakagami H: Preliminary evaluation of antinephritis and radical scavenging activities of glabridin from *Glycyrrhiza glabra*. Fitoterapia 74: 624-629, 2003.

24. Yokota T, Nishio H, Kubota Y and Mizoguchi M: The inhibitory effect of glabridin from licorice extracts on melanogenesis and inflammation. Pigment Cell Res 11: 355-361, 1998.

25. Inoue H, Mori T, Shibata S and Koshihara Y: Modulation by glycyrrhetinic acid derivatives of TPA-induced mouse ear oedema. Br J Pharmacol 96: 204-210, 1989.

26. Gerber B, Scholz C, Reimer T, Briese V and Janni W: Complementary and alternative therapeutic approaches in patients with early breast cancer: A systematic review. Breast Cancer Res Treat 95: 199-209, 2006.

27. Kushman ME, Kabler SL, Ahmad S, Doehmer J, Morrow CS and Townsend AJ: Protective efficacy of hGSTM1-1 against B[a]P and (+)- or (-)-B[a]P-7,8-dihydrodiol cytotoxicity, mutagenicity, and macromolecular adducts in V79 cells coexpressing hCYP1A1. Toxicol Sci 99: 51-57, 2007.

28. Soriano J, García-Díaz M, Mora M, Sagristá ML, Nonell S, Villanueva A, Stockert JC and Cañete M: Liposomal temocene (m-THPPo) photodynamic treatment induces cell death by mitochondria-independent apoptosis. Biochim Biophys Acta 1830: 4611-4620, 2013.

29. Blix ES, Irish JM, Husebekk A, Delabie J, Forfang L, Tierens AM, Myklebust JH and Kolstad A: Phospho-specific flow cytometry identifies aberrant signaling in indolent B-cell lymphoma. BMC Cancer 12: 478, 2012.

30. Wang T, Song X, Zhang Z, Guo M, Jiang H, Wang W, Cao Y, Zhu L and Zhang N: Stevioside inhibits inflammation and apoptosis by regulating TLR2 and TLR2-related proteins in *S. aureus*-infected mouse mammary epithelial cells. Int Immunopharmacol 22: 192-199, 2014.

31. Chen X, Zhang B, Yuan X, Yang F, Liu J, Zhao H, Liu L, Wang Y, Wang Z and Zheng Q: Isoliquiritigenin-induced differentiation in mouse melanoma B16F0 cell line. Oxid Med Cell Longev 2012: 534934, 2012.

32. Livak KJ and Schmittgen TD: Analysis of relative gene expression data using real-time quantitative PCR and the 2(-Delta Delta C(T)) method. Methods 25: 402-408, 2001.

33. Hsu YL, Kuo PL, Lin LT and Lin CC: Isoliquiritigenin inhibits cell proliferation and induces apoptosis in human hepatoma cells. Planta Med 71: 130-134, 2005.

34. Kim DC, Ramachandran S, Baek SH, Kwon SH, Kwon KY, Cha SD, Bae I and Cho CH: Induction of growth inhibition and apoptosis in human uterine leiomyoma cells by isoliquiritigenin. Reprod Sci 15: 552-558, 2008.

35. Jung JI, Chung E, Seon MR, Shin HK, Kim EJ, Lim SS, Chung WY, Park KK and Park JH: Isoliquiritigenin (ISL) inhibits ErbB3 signaling in prostate cancer cells. Biofactors 28: 159-168, 2006.

36. Takahashi T, Takasuka N, Iigo M, Baba M, Nishino H, Tsuda H and Okuyama T: Isoliquiritigenin, a flavonoid from licorice, reduces prostaglandin E2 and nitric oxide, causes apoptosis, and suppresses aberrant crypt foci development. Cancer Sci 95: 448-453, 2004.

37. Zhou GS, Song LJ and Yang B: Isoliquiritigenin inhibits proliferation and induces apoptosis of U87 human glioma cells in vitro. Mol Med Rep 7: 531-536, 2013.

38. Choi JS, Shin S, Jin YH, Yim H, Koo KT, Chun KH, Oh YT, Lee WH and Lee SK: Cyclin-dependent protein kinase 2 activity is required for mitochondrial translocation of Bax and disruption of mitochondrial transmembrane potential during etoposide-induced apoptosis. Apoptosis 12: 1229-1241, 2007.

39. Darvin P, Baeg SJ, Joung YH, Sp N, Kang DY, Byun HJ, Park JU and Yang YM: Tannic acid inhibits the Jak2/STAT3 pathway and induces G1/S arrest and mitochondrial apoptosis in YD-38 gingival cancer cells. Int J Oncol 47: 1111-1120, 2015.

40. Harbour JW, Luo RX, Dei Santi A, Postigo AA and Dean DC: Cdk phosphorylation triggers sequential intramolecular interactions that progressively block Rb functions as cells move through G1. Cell 98: 859-869, 1999.

41. Adon AM, Zeng X, Harrison MK, Sannem S, Kiyokawa H, Kaldis P and Saavedra H: Cdk2 and Cdk4 regulate the centrosome cycle and are critical mediators of centrosome amplification in p53-null cells. Mol Cell Biol 30: 694-710, 2010.

42. Yu L, Ma J, Han J, Wang B, Chen X, Gao C, Li D and Zheng Q: Licochalcone B arrests cell cycle progression and induces apoptosis in human breast cancer MCF-7 Cells. Recent Pat Anticancer Drug Discov 11: 444-452, 2016.

43. Huang J, Lv C, Hu M and Zhong G: The mitochondria-mediate apoptosis of Lepidopteran cells induced by azadirachtin. PLoS One 8: e58499, 2013.

44. Priyadarsini RV, Murugan RS, Sripriya P, Karunagaran D and Nagini S: The neem limonoids azadirachtin and nimbolide induce cell cycle arrest and mitochondria-mediated apoptosis in human cervical cancer (HeLa) cells. Free Radic Res 44: 624-634, 2010.